

Received 11 May 2022, accepted 29 May 2022, date of publication 22 June 2022, date of current version 8 August 2022.

Digital Object Identifier 10.1109/ACCESS.2022.3185257

The Effect of 40 Hz Binaural Beats on Working Memory

LEI WANG¹, WEN ZHANG¹, XINYUE LI¹, AND SHUO YANG¹

State Key Laboratory of Reliability and Intelligence of Electrical Equipment, and the Tianjin Key Laboratory of Bioelectromagnetic Technology and Intelligent Health, Hebei University of Technology, Tianjin 300130, China

Corresponding author: Shuo Yang (sureyang@126.com)

This work was supported in part by the National Natural Science Foundation of China under Grant 51877067.

This work involved human subjects in its research. Approval of all ethical and experimental procedures and protocols was granted by the Biomedical Ethics Committee of Hebei University of Technology (under Application No. HEBUThMEC2021009, and performed in line with the Medical Experiment Ethical Inspection Declaration).

ABSTRACT Binaural beats (BB), in which pure tones are delivered at fixed frequency, seek to influence neural activity during cognitive tasks and induce frequency-following response which can entrain brain rhythms to the frequency of external stimulation. An increasing number of studies have suggested that BB can be used to alter or enhance cognitive processes. This study aimed to explore the effect of 40 Hz binaural beats on working memory. In addition to further verifying whether there was a frequency-following response, changes in microstates were observed, providing new evidence for the effectiveness of binaural beats. 40 healthy volunteers completed visuospatial and verbal working memory tasks when listening to pink noise and 40 Hz binaural beats (R: 440 Hz, L: 400 Hz). The EEG was analyzed in terms of behavioral performance, relative power, Higuchi fractal dimension (HFD) and microstates after BB stimulation. We found that subjects performed better on the working memory task when stimulated by 40 Hz binaural beats, with significantly higher HFD in the temporal and parietal lobes and a significant positive correlation between HFD and relative power in the gamma band, in addition to a significant increase in the duration and coverage of microstate D and a significant decrease in those of microstate A. Our results demonstrate that 40 Hz binaural beats improve working memory, and induce frequency-following responses. Besides, changes in both HFD and microstates are correlated with attention, which may also account for the changes in working memory performance affected by 40 Hz binaural beats.

INDEX TERMS Binaural beats, frequency-following response, microstate, Higuchi fractal dimension.

I. INTRODUCTION

Neuromodulation has emerged as a powerful tool in human neuroscience, and has become integral to the next-generation psychiatric and neurological therapeutics. It can be broadly processed in the human brain using three different stimulation methods: (a) sensory entrainment, (b) invasive electrical entrainment, (c) non-invasive electrical/magnetic entrainment [1]. Each of these methods modulates the activity of neurons and neural networks in which they reside, ultimately inducing changes in specific brain functions. Working memory, an important high-level function of the central nervous system, plays an important role in high-level cognitive activities for many complex tasks, such as comprehension, reading,

and learning, and has become the focus of neuromodulation research.

When two ears hear pure tones of the same intensity but slightly different frequencies simultaneously, the brain receives this frequency difference, which is called binaural beats (BB), and the perceived beat corresponds to the frequency difference of the presented tones. As a sensory entrainment neuromodulation technique, it has a higher safety and cost benefit than other neuromodulation techniques.

BB originate in the inferior colliculus (IC) in the central nervous system (CNS) auditory pathway [2], [3]. By delivering a continuous external stimulus of relatively constant frequency, it can induce frequency-following response, which can entrain brain rhythms to the frequency of the external stimulation [4]. Neuroscientists hypothesize that it may be effective in regulating the activity of the brain circuits responsible for cognitive processing, making it more suitable for

The associate editor coordinating the review of this manuscript and approving it for publication was Rajeeb Dey¹.

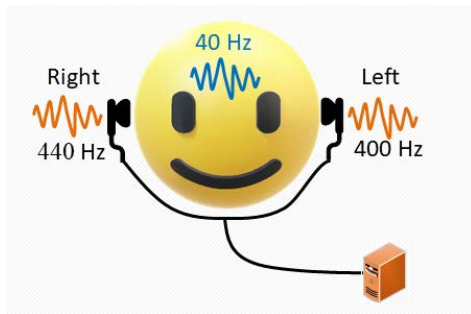


FIGURE 1. 40 Hz binaural beats on a 400 Hz carrier tone generated within the brain.

applications in cognitive function improvement or adjunctive treatment of related cognitive deficit disorders.

Several studies have confirmed that BB have a range of effects on behavior and cognition. For example, Le Scouarnec, Brady [5] and Steven *et al.* suggest that delta and theta band frequencies BB can reduce anxiety, promote deep meditation and increase hypnotic susceptibility; Lane [6] *et al.* demonstrated that beta BB helped increase alertness as well as improve mood; Carlo Lovati's team demonstrated that theta and alpha BB improved migraines [7]; Gerardo Gálvez *et al.* applied 14 Hz BB in a double-blind randomized controlled study in patients with Parkinson's disease (PD) and showed that beta-band frequencies BB can effectively affect brain activity and improve cognitive performance in Parkinson's patients [8]; In addition, previous work in children with attention deficit and hyperactivity disorder (ADHD) has shown that beta BB can also be used in brainwave induction therapy for ADHD and has a facilitative effect on the behavioral performance of children with ADHD [9]; Hessel Engelbregt *et al.* examined the effects of 40 Hz BB and monaural beats (MB) stimulation on attention and working memory in high and low mood participants and found that participants' reaction times were faster when receiving 40 Hz BB, possibly due to the increased speed of attentional processing by gamma-frequency BB [10].

In summary, there is an important feature of the study of the relationship between BB and cognitive function: BB can affect neural oscillations in the brain, thus changing the behavioral performance of subjects, and the frequency of the stimulus can play a crucial role in this process.

The brain exhibits characteristic oscillatory activity, depending on its functional or behavioral state. Among these, gamma frequency oscillations have received much attention from researchers because of their potentially important role in cognitive function [11]–[15]. For example, Laure Verret *et al.* studied human amyloid precursor protein transgenic mice, which simulate key aspects of Alzheimer's disease (AD). Electroencephalographic recordings in mice revealed spontaneous epileptiform discharges primarily during reduced gamma oscillatory activity [16]. In addition, the involvement of gamma-band synchronization in various cognitive paradigms in humans suggested that gamma-frequency

activity has an important role in attention and working memory. Meanwhile, because of its importance in neuronal communication and synaptic plasticity, gamma-frequency oscillatory could provide a key for understanding neuronal processing in both local and distributed cortical networks engaged in complex cognitive functions [14]. Since brain oscillations are central to memory processes, human gamma-band activity provides physiological markers of human attention and memory processes. Therefore, this study selected 40 Hz frequency of the gamma band.

The effects of gamma-frequency BB on cognitive function are currently in a developmental stage. The exact underlying neural mechanisms are unclear, and there are few studies on its effects on tasks related to working memory [17]. Research methods based on gamma-frequency BB include power spectrum analysis, behavioral performance analysis with subjective scale assessment, and brain function connectivity. These research methods lack metrics that can more sensitively detect frequency entrainment and stimulation effects, and do not take full advantage of the nonlinear features and rich spatial information contained in EEG signals. Therefore, we introduced the HFD and microstate analysis methods.

HFD can provide a detailed and precise analysis of subtle changes in EEG after BB stimulation, providing better temporal resolution than spectral analysis. Among the nonlinear methods of analyzing EEG data, fractal dimensions analysis is widely used in various biomedical applications owing to its low computational cost and efficient analysis of nonlinear signal complexity, and it has been found to be effective in the analysis of neuronal disorders [18]. Fractal dimensions quantify the complexity of dynamic signals as the ratio of detailed changes to the scale variation in the signal under consideration. Compared to the Katz and k-nearest neighbor algorithms, Higuchi's algorithm provided the most accurate estimate of the entire range of theoretical FD values [19]. Therefore, we chose HFD as one of the measures to describe the EEG changes after BB stimulation. HFD has been studied under other disease conditions. For example, patients with AD have reduced HFD values in the parietal region compared with healthy controls [20]. HFD can also distinguish between autism spectrum disorder (ASD) and normally developing children [21] and between depressed and normal individuals [22]. Moreover, HFD has been found to be suitable for analyzing various incoherent phenomena such as epilepsy, sleep disorders, and dyslexia. HFD has been successfully applied in different fields of neurophysiology, but the use of HFD in EEG recordings in response to binaural beats is quite novel. Furthermore, the application of HFD in basic research and medical practice demonstrates its advantages and complementarity with existing linear methods. Moreover, the application of HFD in combination with other linear analysis methods shows complementarity and the results are even more reliable and accurate [18]. In this study, relative power was combined with HFD to obtain more accurate and reliable results.

The microstate analysis technique based on scalp electric field topography clustering can make full use of the rich spatial information contained in the EEG signal to fill the gap in past studies, and can reflect the pattern of EEG activity after BB stimulation [23]. EEG microstate analysis began in 1987 with a study by Lehmann *et al.* [24]. They found that the scalp voltage topography of resting-state EEG signals did not change randomly or continuously over time. The topography of the topology remains relatively stable for a certain period (80-120 ms), after which it rapidly switches to another topography that remains relatively stable for a certain period of time [25], [26]. Lehmann *et al.* proposed that the phases in which the topographic map remains in a steady state reflect the basic steps of brain information processing, which constitute the atoms of thought, and are called functional microstates [23], [27]. By microstate analysis of resting-state EEG, four different topographic maps (microstates A, B, C, and D) can explain the vast majority of variation (around 80%) in resting-state EEG signals [28]–[30]. By analyzing the parameters and topographic topology of these four microstate categories, researchers have found that these metrics are associated with numerous factors such as neurological and psychiatric disorders, age, personality traits, and cognitive operations [25], [28], [31]–[36]. Accordingly, microstate analysis seems particularly promising in detecting differences for processing associated with attention, mental states, and reality testing.

In summary, to better explore the neural mechanisms by which gamma-frequency BB affect the physiological state of the brain and to provide new evidence for its effectiveness, we designed visuospatial and verbal working memory tasks, recorded EEG when stimulated by 40 Hz BB and pink noise, and used HFD and microstate analysis methods.

Thus, we propose the following hypotheses: Compared with pink noise, subjects showed (1) significant improvement in cognitive behavior after BB stimulation, (2) significant frequency entrainment in EEG after BB stimulation, (3) significant changes in microstate categories after BB stimulation.

II. MATERIALS AND METHOD

All the volunteers completed an informed consent form before participating in the experiment. Ethical approval for the study was granted by the Biomedical Ethics Committee of Hebei University of Technology (approval number:

HEBUTHMEC2021009). All experimental dataset involved in this study were collected by ourself.

A. PARTICIPANTS

We recruited 40 healthy participants (18 females, 22 males; mean age = 22.64 years, SD = 2.60 years) who reported no history of hearing, color weakness, color blindness or neurological disorder.

B. STIMULI

It has been recommended that the afferent neural representation of stimulus is better in the neighborhood of 300-600 Hz

than at higher or lower frequencies [37], [38]. Thus, 400 Hz was chosen as the carrier frequency for the stimuli to present 40 Hz BB (L:400 Hz; R:440 Hz).

Many teams have used white noise, pink noise or blank tape as control groups in their studies and found no significant differences in the experimental results produced by these control groups [8], [10], [39]–[42]. The results of the significance analysis of the scores of the evaluation indexes of different noises by Wu *et al.* showed that there was no significant difference between the subjective evaluation scores of pink noise and white noise. This indicated that the subjects' subjective perceptions of pink and white noise were approximately the same [43], while the interference and annoyance of pink noise were slightly lower than those of white noise. Therefore, pink noise was used as the control in this experiment. The stimulus was delivered to each participant via Huawei®AM115 over-ear headphones.

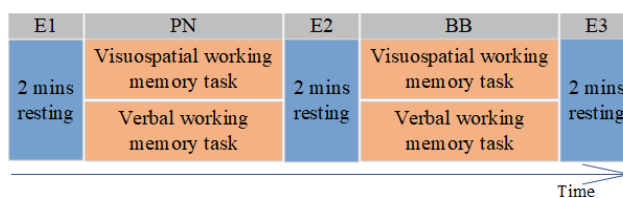


FIGURE 2. The schematic representation of experiment structure.

C. EXPERIMENTAL PROTOCOL

The experiment consisted of two main parts. A visuospatial working memory task and a verbal working memory task were performed successively when stimulated by pink noise (PN) and 40 Hz binaural beats (BB). It has been demonstrated that BB continue to have a persistent effect on cognitive behavior as well as EEG for a while after stimulation; Therefore, PN was arranged before BB in this experiment.

Before and after each part, the EEG was collected with eyes closed for two minutes. Thus, the experiment encompassed 5 blocks (E1, PN, E2, BB, E3) with a total duration about 50 mins (Fig.2).

1) VISUOSPATIAL WORKING MEMORY TASK PARADIGM: DELAYED MATCH-TO-SAMPLE VISUOSPATIAL TASK

Delayed match-to-sample task allows each phase of working memory (encoding period, maintenance period, and retrieval period) to be completely divided by time, facilitating the phasing of working memory, which is highly utilized in research [44]. As shown in Fig.3, after encoding the initial image, volunteers were instructed to retain the image without further input during working memory maintenance. During retrieval, subjects were asked to compare the retained image with the current image and point out whether they matched. The difficulty will gradually increase during the process, slowly transitioning from delayed match-to-sample of two color-blocks to delayed match-to-sample of five color blocks.

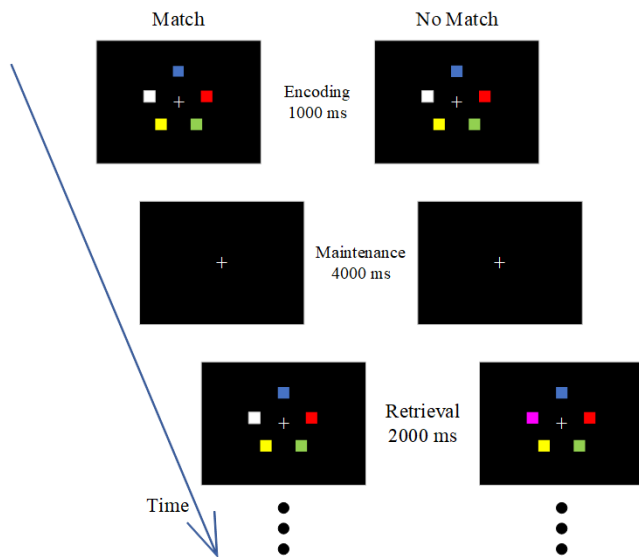


FIGURE 3. The schematic representation of delayed match-to-sample visuospatial working memory task.

2) VERBAL WORKING MEMORY TASK PARADIGM: WORD LIST RECALL TASK

The word list recall task in the present study consisted of two groups of words (Source from Modern Chinese Corpus, word frequency between 45% and 55%). Each word list contained 15 words items, and all words were presented for 2 s. The recall period began two minutes after the end of the last word. Subjects were required to write down each word they could remember in any order.

D. EXPERIMENT APPARATUS AND EEG RECORDING

We used earphones AM115 to present the stimuli. EEG data were recorded using a 64-channel Quick-cap system (Compumedics, Neuroscan) at 1000 Hz sampling rate. The impedance of all electrodes was $< 10 \text{ k}\Omega$.

Data were re-referenced to the binaural mastoid. Due to the fact that induced gamma-band activity in scalp-recorded EEG data usually appears as bursts of high frequency, approximately 30-80 Hz, oscillatory activity [45]–[48], and Finite Impulse Response (FIR) filter is suitable for extracting specific frequency intervals with sensitive and realistic filtering parameters [49], we used 6 independent FIR filters to obtain full-band (1-80 Hz), delta-band (1-4 Hz), theta-band (4-8 Hz), alpha-band (8-13Hz), beta-band (13-30 Hz) and gamma-band (30-80 Hz) frequency intervals. And the power line noise was removed via the 50 Hz bandstop filters. At the same time, to ensure the integrity of the data and the reliability of the results, this study did not apply downsampling. In addition, a semi-automatic procedure, based on Independent Component Analysis (ICA), was applied to identify and remove ocular, cardiac and muscular artefacts. Finally, a threshold of $\pm 100 \mu\text{V}$ was used to exclude artifacts with high amplitudes.

E. SIGNAL PROCESSING

1) RELATIVE POWER

Fast Fourier transform (FFT) was conducted on each selected signal. Relative power (RP) of delta, theta, alpha, beta and gamma oscillations were assessed for statistical analysis. The use of relative power can better eliminate the impact caused by fluctuations of the total energy of EEG waves and highlight the proportion of power in a certain frequency band in the total power.

2) HFD

The method to calculate the fractal dimension of in-plane curves was proposed by Higuchi in 1988. A fractal function or signal can be analyzed as a time series $x(1), x(2), \dots, x(N)$ where N is the number of data points in the original signal. From the starting time series, a new self-similar time series X_k^m is computed as:

$$X_k^m = [x(m), x(m+k), x(m+2k), \dots, x(m + \text{int}[\frac{N-m}{k}]k)] \quad (1)$$

for $m = 1, 2, \dots, k$, and $k = 1, 2, \dots, k_{max}$, where m and k are integers. The length of the curve $L_m(k)$ formed by X_k^m is computed as follows:

$$L_m(k) = \frac{\sum_{i=1}^{\text{int}[\frac{N-m}{k}]} |x(m+ik) - x(m+(i-1)k)| \frac{N-1}{\text{int}[\frac{N-m}{k}]k}}{k} \quad (2)$$

$L_m(k)$ was averaged for all m forming the mean value of the curve length $L(k)$ for each $k = 1, \dots, k_{max}$ as:

$$L(k) = \frac{\sum_{m=1}^k L_m(k)}{k} \quad (3)$$

The slope of least squares linear best fit from the plot of $\ln(L(k))$ versus $\ln(1/k)$ gives the HFD:

$$HFD = \ln(L(k))/\ln(1/k) \quad (4)$$

For each volunteer, HFD was calculated for each channel separately. The k_{max} calculation for each channel is derived on the basis of the saturation range of the HFD [21].

3) MICROSTATE ANALYSIS

Currently, researchers mainly use two spatial clustering algorithms: K-means clustering algorithm, atomize and agglomerate hierarchical clustering (AAHC) technique [50]. Some researchers have compared two algorithms and found their performance is comparable [51], so we used AAHC clustering algorithm with the following steps.

(1) Calculate the global field power (GFP) of each topographic map. Because the topographic maps with higher GFP usually have higher relative stability and signal-to-noise ratio, only the topographic maps located at the peak of GFP are used

as the “original map” in clustering.

$$GFP(t) = \sqrt{\frac{\sum_{i=1}^N (\mu_i - \bar{\mu})^2}{N}} \quad (5)$$

where N denotes the total number of electrodes, μ_i is the voltage value of the i th electrode at moment t , $\bar{\mu}$ is the average voltage value of all electrodes at that moment.

(2) Each original map was assigned to a unique category.

(3) Calculate the spatial correlation coefficient of each template graph with each original graph separately. All topographic maps in this category are independently reassigned to the category with the highest spatial correlation coefficient.

(4) AAHC iterates by removing one category at a time, until all original maps are combined into 4 microstate categories.

Common indices of resting-state EEG microstate analysis in research include: Duration (mean duration of a microstate class), Occurrence (occurrence rate per second of a microstate class), Coverage (time coverage of a microstate class) and TP (transition probability between microstate class) [26], [34]. The microstate analysis was computed using MST1.0 plugins in eeglab toolbox.

4) STATISTICAL ANALYSIS

Behavioral data from different blocks were statistically analyzed using matched samples t-test to analyze the effect of BB on the behavioral performance of working memory.

To examine how the different condition impact the EEG feature, repeated measures analysis of variance (ANOVA) was computed for each microstate parameter (coverage, occurrence and duration and TP), HFD and RP. Repeated measures ANOVA performed the statistical tests at the significance level of $\alpha = 0.05$.

III. RESULT

A. BEHAVIORAL PERFORMANCE

1) DELAYED MATCH-TO-SAMPLE TASK

The accuracy and response time of the different workloads in PN block and BB block were statistically analyzed by matched samples t-test. Only the total accuracy was statistically different ($P = 0.010 < 0.05$), and the total accuracy was larger in BB block than PN block (Fig.4).

2) WORD LIST RECALL TASK

We calculated the number and scores of recalled words separately. As for calculating the score, each word position had its own weighting points as follows: 1 point for each of the 1 to 3 positions at the beginning and end of the list; 3 points for each of the 4 to 6 positions at the beginning and end of the list; and 5 points for each of the 7 to 9 positions in the list.

The mean and standard deviations (SD) of the number and scores of recalled words under different acoustic stimulation are as Table 1 showed. The number of recalled words in PN block and BB block were statistically analyzed by matched samples t-test and found to be statistically different

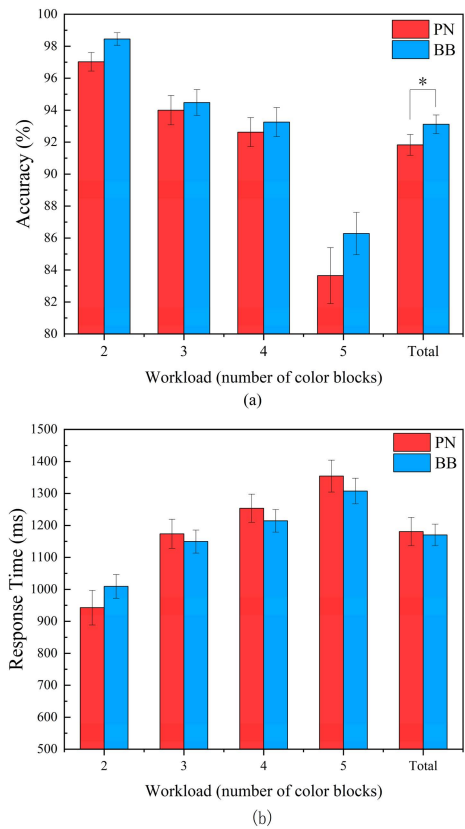


FIGURE 4. Behavioral performance of delayed match-to-sample visuospatial task. (a) The accuracy of the different workloads in PN block and BB block. (b) the response time of the different workloads in PN block and BB block (mean \pm standard error). Asterisks indicates the t-test was significant ($p < 0.05$).

($p < 0.001$). Similarly, the scores of recalled words in PN block and BB block were statistically analyzed by matched samples t-test and also revealed a significant difference ($P = 0.006$).

B. RELATIVE POWER

The repeated-measure ANOVA revealed no significant changes in any relative power of different frequency bands in E1, E2 and E3 blocks ($p > 0.05$). As shown in Fig.5, the relative power in the occipital, parieto-occipital and temporal lobes increased a little in the E3 block, but there was no significant difference.

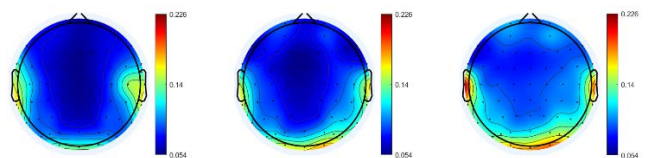


FIGURE 5. The relative power topography of gamma frequency band at each block.

TABLE 1. Results of behavioral performance in word list recall task.

Results of the word list recall task	Stimulation	Mean	SD	Results of the matched samples t-test
Number of recall word	PN	7.73	2.16	$t=-4.507, p<0.001$
	BB	9.38	2.529	
Score of recall word	PN	18.88	6.775	$t=-2.883, p=0.006$
	BB	22.6	8.152	

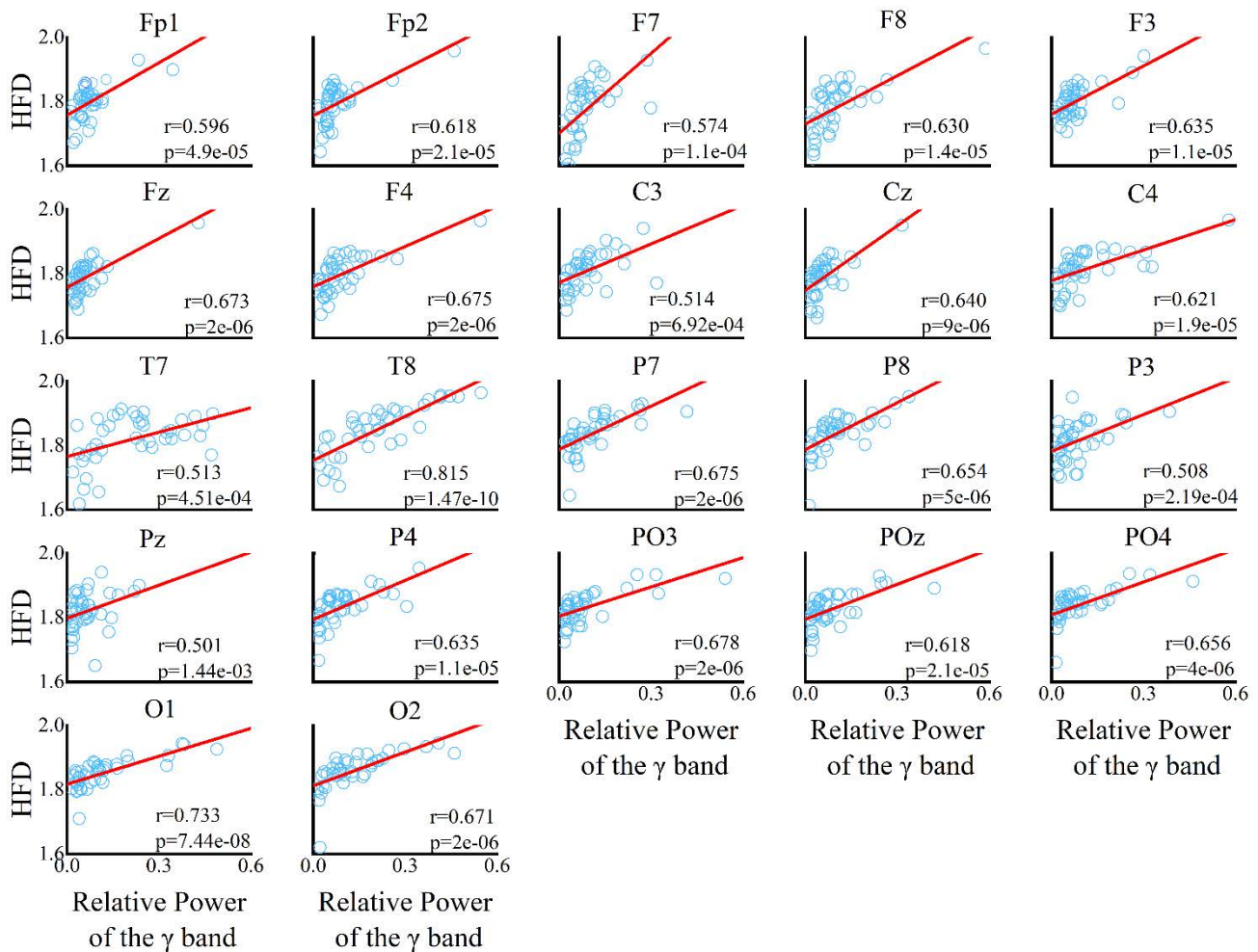


FIGURE 6. Scatter plots of HFD and relative power of the gamma band in the electrodes of the prefrontal, frontal, central, temporal, parietal, parietal-occipital and occipital lobes, along with the best line fitted to the data through the least square method. There was significant positive correlation between HFD and relative power of the gamma band in all the electrodes of seven lobes. In each plot, r represents Pearson's correlation coefficient, while p is the p -value obtained in the Pearson's correlation test.

C. HFD

We calculated the HFD for each channel of each block for each individual. In addition, Pearson's correlation test was performed in order to investigate whether there is a relationship between the HFD and the relative power of the gamma band. The results (Fig.6) found that the HFD of each channel had a significant positive correlation with the relative power of the gamma band. This presentation of the cross-correlation between them is also pretty novel.

As it is shown in Fig.7, there were significant differences between the HFD corresponding to the different blocks in the temporal ($F(1.774,69.194) = 5.139, p = 0.011$) and parietal ($F(1.499,58.448) = 5.294, p = 0.14$) lobes.

Results indicated that all the E3 blocks had significantly higher HFD than the E1 and E2 block in the temporal and parietal lobes. To deeply investigate the changes of HFD in channels, electrodes in these regions were individually put to the statistical analysis. Significant differences were observed

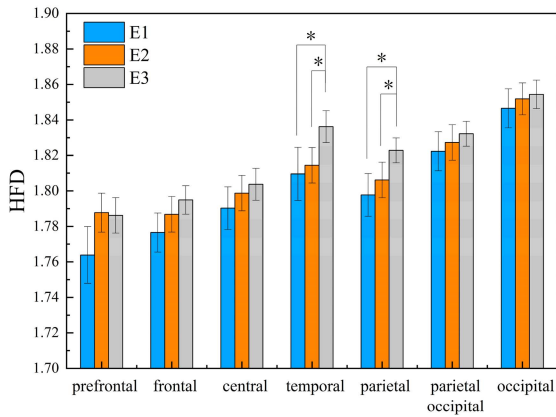


FIGURE 7. Group means of the HFD of seven brain regions in E1, E2, E3 block (mean ± standard error). Asterisks indicates the ANOVA was significant ($p < 0.05$).

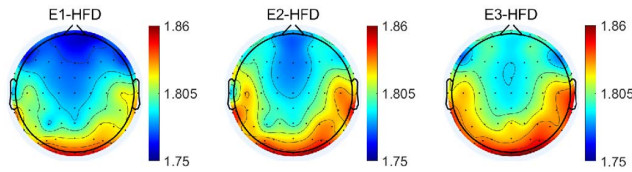


FIGURE 8. The topographic distribution of HFD in each block.

in T7 ($F(2,78) = 7.181, p = 0.001$), P3 ($F(1.448,56.465) = 3.805, p = 0.027$), and Pz ($F(1.269,49.493) = 7.886, p = 0.004$). Results revealed that E3 blocks had significantly higher HFD than the other block in T7, P3 and P7 (Fig. 8).

D. MICROSTATE ANALYSIS

The four grand mean microstate classes (Fig.9) extracted from resting EEG of the different blocks in E1, E2 and

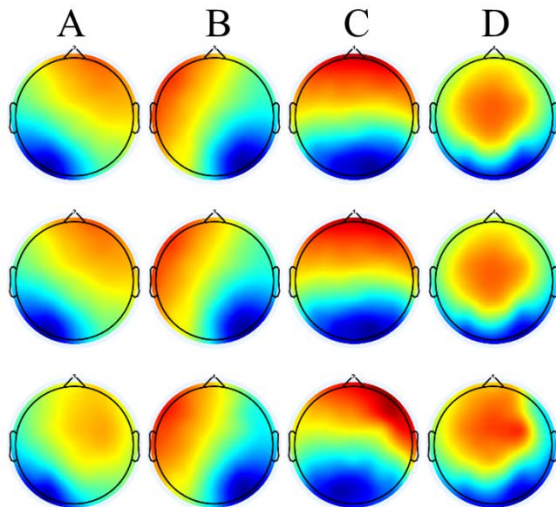


FIGURE 9. Microstate EEG topography (Upper: E1 block; Middle: E2 block; Lower: E3 block). All of them are highly similar to the four types of classical microstate topographies from previous studies: microstate A has a topographic centre of gravity in the left frontal and right parieto-occipital lobes, microstate B has a topographic centre of gravity in the left parieto-occipital and right frontal lobes, microstate C has a topographic centre of gravity in the central frontal and parieto-occipital lobes and microstate D has a topographic centre of gravity in the frontal and central regions.

E3 were very similar to the 4 classes from the normative database. It is important to note that the polarity of each raw map needs to be ignored in the topographic clustering analysis of resting-state EEG signals. And variance ratios of the 4 kinds of topographic map interpretations were all between 67% and 82%.

We performed repeated measures ANOVA on the microstate time series parameters of all subjects, using Greenhouse-Geisser sphericity correction and Bonferroni correction for multiple comparisons (Fig.10).

Duration of microstate A was significantly different ($F(1.584,61.770) = 8.642, P = 0.001$) in E1, E2 and E3 block. And it in E3 block was significantly smaller than the other two blocks ($E3 < E1: p = 0.010; E3 < E2: p = 0.007$); Coverage of microstate A was significantly different ($F(2,78) = 18.516, P < 0.001$) in E1, E2 and E3 block. Moreover, it in E3 block was significantly smaller than the other two blocks ($E3 < E1: p < 0.001; E3 < E2: p < 0.001$).

Duration of microstate D was significantly different ($F(1.592,62.070) = 6.880, P = 0.004$) in E1, E2 and E3 block. And it in E3 block was significantly larger than E1 block ($E3 > E1: p = 0.012$); Also, coverage of microstate D was significantly different ($F(1.789,69.761) = 14.504, P < 0.001$) in E1, E2 and E3 block. Besides, it in E3 block was significantly bigger than the other two blocks ($E3 > E1: p < 0.001; E3 > E2: p = 0.010$).

In terms of TP_{BA} (Transition Probability of microstate B to microstate A), there was significant difference among E1, E2 and E3 block ($F(2,78) = 15.039, P < 0.001$). Moreover, it in E3 block was significantly smaller than the other two blocks ($p < 0.001$); For TP_{CA} , there was significant difference among E1, E2 and E3 block ($F(2,78) = 28.962, P < 0.001$). In addition, it in E3 block was significantly smaller than the other two blocks ($p < 0.001$); In terms of TP_{DA} , there was significant difference among E1, E2 and E3 block ($F(1.759,68.610) = 8.280, P = 0.001$). Also, it in E3 block was significantly smaller than the other two blocks ($E3 < E1: p = 0.023; E3 < E2: P = 0.004$); As for TP_{BD} , there was significant difference among E1, E2 and E3 block ($F(2,78) = 8.408, P < 0.001$). And, it in E3 block was significantly larger than the other two blocks ($E3 > E1: p = 0.001; E3 > E2: p = 0.013$); As for TP_{CD} , there was significant difference among E1, E2 and E3 block ($F(1.660,64.725) = 11.177, P < 0.001$). Furthermore, it in E3 block was significantly larger than E1 block ($E3 > E1: p = 0.001$).

IV. DISCUSSION

As expected, we observed significant differences in behavioral performance and EEG characteristics after BB stimulation compared with pink noise.

A. BEHAVIORAL PERFORMANCE

Compared to pink noise, the results of both the visuospatial working memory task and the verbal working memory task were significantly different when stimulated by BB. This indicates that 40 Hz BB can effectively improve the subjects' working memory performance and enhance cognitive levels.

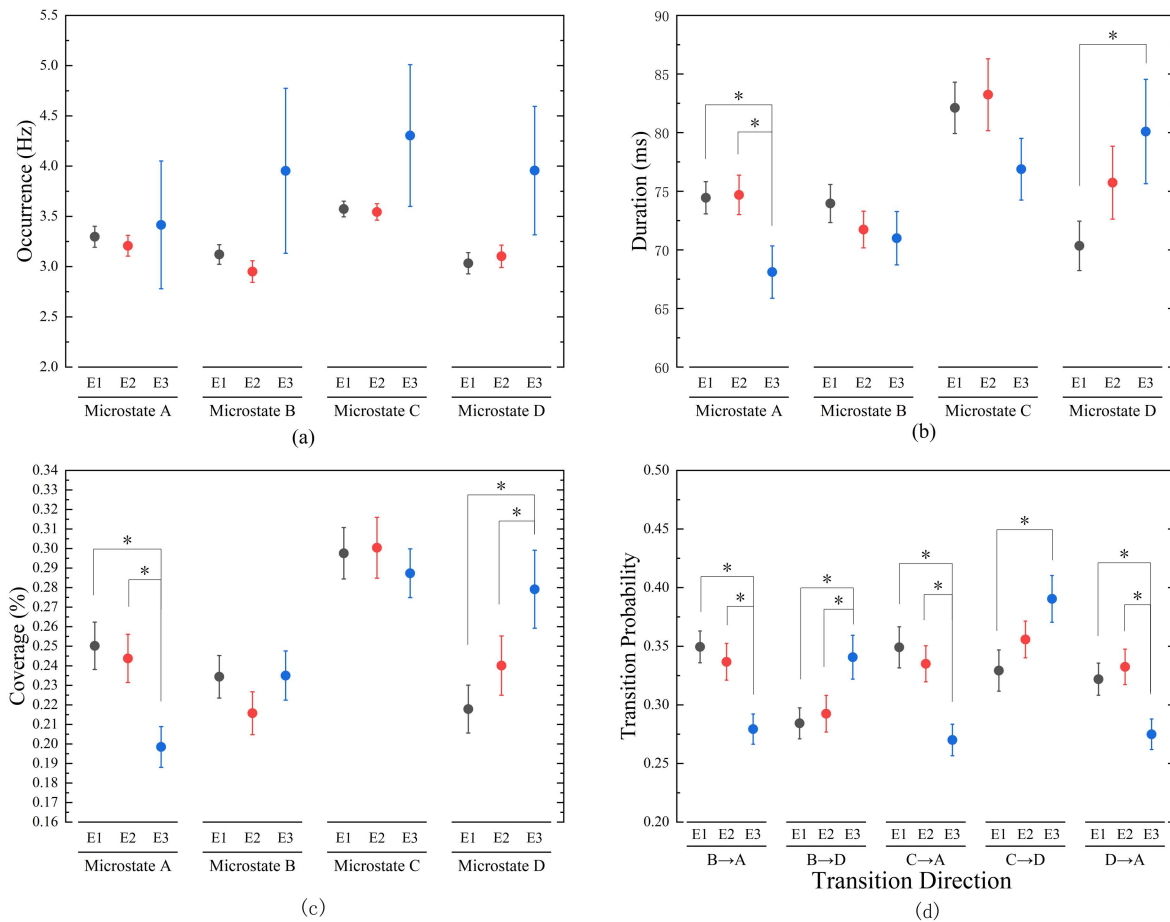


FIGURE 10. Microstate parameters (mean and standard error) in E1, E2 and E3 block. (a) Occurrence, (b) Duration, (c) Coverage, and (d) TP. Limited to space, the TP map only draws part of the data with differences between groups (Black represents E1 block, red represents E2 block, blue represents E3 block; Asterisks indicates the ANOVA was significant, $p < 0.05$).

This is consistent with the findings of Friedrich *et al.* [52], who showed that stimulation at 40 Hz enhances memory capacity. However, gamma stimulation at 37.5 Hz did not modulate memory recall accuracy in Chen *et al.*'s study [53]. This may be because 40 Hz is the ideal spike-time-dependent plasticity (STDP) in the human visual cortex during memory encoding, while 37.5 Hz is not. It refers to the fact that synaptic plasticity has been shown to be heavily dependent on the time delay between upstream and downstream neuronal firing. A rat study found that synaptic plasticity is highly sensitive to the timing of firing and that spikes must co-occur within a time window of approximately 25 ms (corresponding to a gamma frequency of 40 Hz) to facilitate synaptic modifications [54]. This is thought to underlie memory formation. This means that 40 Hz oscillations may modulate memory content during the memory encoding phase, in line with the time window of STDP, and therefore improve working memory performance.

B. RELATIVE POWER

The results showed that the relative power of gamma was not significantly different at all electrodes which is consistent

with reports of similar null effects following exposure to theta [4] and alpha [53] binaural beats.

However, the lack of significant difference in relative power alone does not deny that BB do not produce frequency entrainment, and it has been reported that HFD can replace relative power as a tool to verify frequency entrainment and is more sensitive than relative power. Therefore, we also analyzed the variation in HFD.

C. HFD

The results showed that HFD was significantly and positively correlated with gamma relative power, and 40 Hz BB increased the HFD. Besides, this change had a significant influence on the temporal and parietal lobes, especially at electrodes T7, P3, and Pz.

The temporal lobe is responsible for memory storage and is associated with hearing. The left temporal lobe, where T7 is located, contains linguistic analysis areas of the brain, such as Broca's area (syntactic processing and speech production) and Wernicke's area (auditory association and speech comprehension) [56]. Moreover, there is evidence that significant activation of T7 plays an important role in memory

retrieval [57]. P3 is close to the superior parietal and intraparietal sulcus lobes, as the basic structure of the dorsal attentional network. It has high potential to be the most sensitive electrode in the dorsal attentional network [58]. In a study that used fractal dimension to distinguish between relaxation and attention, P3 was found to be the best spot for measuring attention [59]. The precuneus (Pz) is an important structure involved in processing visual image information during recall. Focused attention enhances its activity. In addition, the parietal cortex is thought to play an important role in different memory systems, such as the retrieval of visuospatial working memory [60]. These facts explain why the changes in HFD were stronger in these electrodes.

Our study, for the first time, demonstrated that for each of the electrodes in the aforementioned lobes, there was significant positive correlation between the relative power of the gamma band and HFD. In other words, the more brain entrainment BB caused, the more HFD was obtained, which is equivalent to greater EEG complexity.

The reason may lie in the fact that BB deal with cognitive aspects, such as attention [61], focusing [62] and memory [17], [63], [64]. In particular, BB mobilize more attentional resources and perceptual arousal (i.e., more complex) brain responses [65], with an increased distribution of cortical activity.

On the other side, in this study, the EEG signal had a fractal behavior on a large frequency band that produced a spreading of signal energy with a corresponding higher fractal dimension value [66].

D. MICROSTATE ANALYSIS

Previous studies have shown that microstates are thought atoms that can represent the underlying cognitive processes in different states and tasks [67]–[70]. To the best of our knowledge, this study is the first to propose EEG microstates to study the neuromodulatory mechanisms of 40 Hz binaural beats. And our results showed that microstates could be used as novel markers to reveal the neuromodulatory effects of 40 Hz binaural beats. First, compared to pink noise, after 40 Hz BB stimulation the main findings were a significant increase in the duration and coverage of microstate D and a significant decrease in microstate A. Second, the functional significance of the four microstates and their interactions have not been fully determined, but many studies agree that the functions of microstates A, B, C, and D are correlated with auditory, visual, default mode, and attention, respectively, in the fMRI resting-state networks (RSN) [35], [71], [72].

Microstate A was related to activation of the bilateral superior temporal gyrus regions and middle temporal gyrus regions that are associated with speech processing [71]. Cai *et al.* demonstrated that the duration of microstate A in patients with tinnitus was significantly increased [73]. These results are similar to the findings of Milz *et al.*, who found that verbal cognition was negatively associated with the duration of microstate A [67]. That is, the experimental results of the present study suggest that the requirement for

auditory processing may be reduced after 40 Hz binaural beats stimulation, but does not diminish the ability of the processing system to store linguistic information, thus reducing the appearance of microstate.

Microstate D correlates with signals in the right lateral dorsal and ventral regions of the frontal and parietal cortices. These regions roughly correspond to the central executive network [71]. The network is involved in active manipulation and maintenance of attention, decision-making, and working memory [74]. Marina *et al.* observed a positive association between the duration of microstate D and vigilance level [75]. Moreover, the most robust finding, confirmed in a recent meta-analysis [29], is a decrease in microstate D in patients with schizophrenia [27] or at risk of developing schizophrenia [74], [76], a disequilibrium that is normalized when patients are treated with antipsychotic medication [77] and with rTMS [78]. These findings correspond well with the interpretation that microstate D reflects attention and cognitive control.

In the present study, the duration and coverage of microstate D strongly increased after binaural beats stimulation. This could reflect achievement on the task, which implies that activation of the central executive network leads to improved attention and better performance on the working memory task. It may reveal a new perspective on the effect of binaural beats on cognitive behavioral changes found in previous studies [3], [4], [37], [38].

Besides, in patients with schizophrenia, major depressive disorder [79], or Huntington's disease, there is converging evidence that microstate D, and functions assumingly associated with it, are reduced but increased in microstate A.

Consequently, 40 Hz BB stimulation effectively influences microstate A and microstate D may constitute a treatment option with a potential positive effect on these psychiatric disorders.

V. CONCLUSION

Our results show that there is a significant increase in HFD in the temporal and parietal lobes after 40 Hz binaural beats stimulation, and prove that there is a significant positive correlation between the relative power in the gamma band and HFD. In other words, it was further verified that 40 Hz binaural beats could induce frequency-following response. HFD can replace relative power as a detection tool to verify brain frequency entrainment, and it is more rapid and sensitive. Thus, HFD can be used for real-time detection of stimulation effects in the future, for example, to recognize user's mental state changes when performing the steady-state visual evoked potential-brain-computer interface task [80]. At the same time, the microstate A parameter was significantly reduced and the microstate D parameter was significantly increased after 40 Hz binaural beats stimulation. Changes in both HFD and microstate parameters were correlated with hearing and attention, which may explain the behavioral changes in working memory affected by binaural beats.

In the future, it may be possible to use 40 Hz binaural beats to assist in the treatment of related diseases such as schizophrenia, major depressive disorder or Huntington's disease. Moreover, it is possible to apply 40 Hz binaural beats in real-life situations where high levels of performance in working memory-related events can be expected.

However, we found that the computational burden and run time of HFD are more than that of relative power. Therefore, the development of new methods for fractal dimension estimation can solve the computational speed problem, and thus create better measures for detecting brain frequency entrainment that can be used for real-time applications. Besides, due to the limitation of experimental equipment, we used EEG, which is the most widely used, for this study. In the future, if other brain imaging techniques (such as fMRI or PET) can be used, more comprehensive research results can be obtained.

REFERENCES

- [1] S. Hanslmayr, N. Axmacher, and C. S. Inman, "Modulating human memory via entrainment of brain oscillations," *Trends Neurosci.*, vol. 42, no. 7, pp. 485–499, Jul. 2019.
- [2] D. C. Fitzpatrick, J. M. Roberts, S. Kuwada, D. O. Kim, and B. Filipovic, "Processing temporal modulations in binaural and monaural auditory stimuli by neurons in the inferior colliculus and auditory cortex," *J. Assoc. Res. Otolaryngol.*, vol. 10, no. 4, p. 579, Jun. 2009.
- [3] B. H. Scott, B. J. Malone, and M. N. Semple, "Representation of dynamic interaural phase difference in auditory cortex of awake rhesus macaques," *J. Neurophysiol.*, vol. 101, no. 4, pp. 1781–1799, Apr. 2009.
- [4] H. Wahbeh, C. Calabrese, and H. Zwickey, "Binaural beat technology in humans: A pilot study to assess psychologic and physiologic effects," *J. Alternative Complementary Med.*, vol. 13, no. 1, pp. 25–32, Jan. 2007.
- [5] R. P. Le Scouarnec, R. M. Poirier, J. E. Owens, J. Gauthier, A. G. Taylor, and P. A. Foresman, "Use of binaural beat tapes for treatment of anxiety: A pilot study of tape preference and outcomes," *Alternative Therapies Health Med.*, vol. 7, no. 1, pp. 58–63, Jan. 2001.
- [6] J. D. Lane, S. J. Kasian, J. E. Owens, and G. R. Marsh, "Binaural auditory beats affect vigilance performance and mood," *Physiol. Behav.*, vol. 63, no. 2, pp. 249–252, Jan. 1998.
- [7] C. Lovati, A. Freddi, F. Muzio, and L. Pantoni, "Binaural stimulation in migraine: Preliminary results from a 3-month evening treatment," *Neurolog. Sci.*, vol. 40, no. S1, pp. 197–198, Mar. 2019.
- [8] G. Gálvez, M. Recuero, L. Canuet, and F. Del-Pozo, "Short-term effects of binaural beats on EEG power, functional connectivity, cognition, gait and anxiety in Parkinson's disease," *Int. J. Neural Syst.*, vol. 28, no. 5, Jun. 2018, Art. no. 1750055.
- [9] H. Wang, "Development and application of music therapy aids for children with disabilities," Ph.D. dissertation, Dept. Educ., East China Normal Univ., Shanghai, China, 2016.
- [10] H. Engelbregt, N. Meijburg, M. Schulten, O. Pogarell, and J. B. Deijen, "The effects of binaural and monaural beat stimulation on cognitive functioning in subjects with different levels of emotionality," *Adv. Cognit. Psychol.*, vol. 15, no. 3, pp. 199–207, Sep. 2019.
- [11] P. Fries, "Neuronal gamma-band synchronization as a fundamental process in cortical computation," *Annu. Rev. Neurosci.*, vol. 32, pp. 309–324, Jul. 2009.
- [12] P. Fries, D. Nikolić, and W. Singer, "The gamma cycle," *Trends Neurosci.*, vol. 30, no. 7, pp. 309–316, Jul. 2007.
- [13] L. M. Ward, "Synchronous neural oscillations and cognitive processes," *Trends Cognit. Sci.*, vol. 7, no. 12, pp. 553–559, Dec. 2003.
- [14] O. Jensen, J. Kaiser, and J.-P. Lachaux, "Human gamma-frequency oscillations associated with attention and memory," *Trends Neurosci.*, vol. 30, no. 7, pp. 317–324, Jul. 2007.
- [15] C. S. Herrmann, M. H. J. Munk, and A. K. Engel, "Cognitive functions of gamma-band activity: Memory match and utilization," *Trends Cognit. Sci.*, vol. 8, no. 8, pp. 347–355, Aug. 2004.
- [16] L. Verret, E. O. Mann, G. B. Hang, A. M. I. Barth, I. Cobos, K. Ho, N. Devidze, E. Masliah, A. C. Kreitzer, I. Mody, L. Mucke, and J. J. Palop, "Inhibitory interneuron deficit links altered network activity and cognitive dysfunction in Alzheimer model," *Cell*, vol. 149, no. 3, pp. 708–721, Apr. 2012.
- [17] N. Jirakittayakorn and Y. Wongsawat, "Brain responses to 40-Hz binaural beat and effects on emotion and memory," *Int. J. Psychophysiol.*, vol. 120, pp. 10–96, Oct. 2017.
- [18] S. Kesić and S. Z. Spasić, "Application of Higuchi's fractal dimension from basic to clinical neurophysiology: A review," *Comput. Methods Programs Biomed.*, vol. 133, pp. 55–70, Sep. 2016.
- [19] G. E. Polychronaki, P. Y. Ktonas, S. Gatzonis, A. Siatouni, P. A. Avvestas, H. Tsekou, D. Sakas, and K. S. Nikita, "Comparison of fractal dimension estimation algorithms for epileptic seizure onset detection," *J. Neural Eng.*, vol. 7, no. 4, Aug. 2010, Art. no. 046007.
- [20] A. H. Al-Nuaimi, E. Jammeh, L. Sun, and E. Ifeachor, "Higuchi fractal dimension of the electroencephalogram as a biomarker for early detection of Alzheimer's disease," in *Proc. 39th Annu. Int. Conf. IEEE Eng. Med. Biol. Soc. (EMBC)*, Jul. 2017, pp. 2320–2324.
- [21] M. Radhakrishnan, D. Won, T. A. Manoharan, V. Venkatachalam, R. M. Chavan, and H. D. Nalla, "Investigating electroencephalography signals of autism spectrum disorder (ASD) using Higuchi fractal dimension," *Biomed. Eng./Biomedizinische Technik*, vol. 66, no. 1, pp. 59–70, Aug. 2020.
- [22] B. Hosseinifard, M. H. Moradi, and R. Rostami, "Classifying depression patients and normal subjects using machine learning techniques and non-linear features from EEG signal," *Comput. Methods Programs Biomed.*, vol. 109, no. 3, pp. 339–345, 2013.
- [23] A. Khanna, A. Pascual-Leone, C. M. Michel, and F. Farzan, "Microstates in resting-state EEG: Current status and future directions," *Neurosci. Biobehav. Rev.*, vol. 49, pp. 105–113, Feb. 2015.
- [24] D. Lehmann, H. Ozaki, and I. Pal, "EEG alpha map series: Brain microstates by space-oriented adaptive segmentation," *Electroencephalogr. Clin. Neurophysiol.*, vol. 67, no. 3, pp. 271–288, Sep. 1987.
- [25] T. Koenig, L. Prichep, D. Lehmann, P. V. Sosa, E. Braeker, H. Kleinlogel, R. Isenhardt, and E. R. John, "Millisecond by millisecond, year by year: Normative EEG microstates and developmental stages," *NeuroImage*, vol. 16, no. 1, pp. 41–48, May 2002.
- [26] C. M. Michel and T. Koenig, "EEG microstates as a tool for studying the temporal dynamics of whole-brain neuronal networks: A review," *NeuroImage*, vol. 180, pp. 577–593, Oct. 2018.
- [27] D. Lehmann, P. L. Faber, S. Galderisi, W. M. Herrmann, T. Kinoshita, M. Koukkou, A. Mucci, R. D. Pascual-Marqui, N. Saito, J. Wackermann, G. Winterer, and T. Koenig, "EEG microstate duration and syntax in acute, medication-naïve, first-episode schizophrenia: A multi-center study," *Psychiatry Res., Neuroimage*, vol. 138, no. 2, pp. 141–156, Feb. 2005.
- [28] F. Gao, H. Jia, X. Wu, D. Yu, and Y. Feng, "Altered resting-state EEG microstate parameters and enhanced spatial complexity in male adolescent patients with mild spastic diplegia," *Brain Topography*, vol. 30, no. 2, pp. 233–244, Mar. 2017.
- [29] K. Rieger, L. Diaz Hernandez, A. Baenninger, and T. Koenig, "15 years of microstate research in schizophrenia—Where are we? A meta-analysis," *Frontiers Psychiatry*, vol. 7, p. 22, Feb. 2016.
- [30] D. Van De Ville, J. Britz, and C. M. Michel, "EEG microstate sequences in healthy humans at rest reveal scale-free dynamics," *Proc. Nat. Acad. Sci. USA*, vol. 107, no. 42, pp. 18179–18184, Oct. 2010.
- [31] J. Britz, L. D. Hernández, T. Ro, and C. M. Michel, "EEG-microstate dependent emergence of perceptual awareness," *Frontiers Behav. Neurosci.*, vol. 8, p. 163, May 2014.
- [32] C. Andreou, P. L. Faber, G. Leicht, D. Schoettle, N. Polomac, I. L. H. Opatz, D. Lehmann, and C. Mulert, "Resting-state connectivity in the prodromal phase of schizophrenia: Insights from EEG microstates," *Schizophr Res.*, vol. 152, nos. 2–3, pp. 513–520, Feb. 2014.
- [33] F. Hatz, M. Hardmeier, N. Benz, M. Ehrensperger, U. Gschwandtner, S. Rüegg, C. Schindler, A. U. Monsch, and P. Fuhr, "Microstate connectivity alterations in patients with early Alzheimer's disease," *Alzheimer's Res. Therapy*, vol. 7, no. 1, pp. 1–11, Dec. 2015.
- [34] F. Schlegel, D. Lehmann, P. L. Faber, P. Milz, and L. R. R. Gianotti, "EEG microstates during resting represent personality differences," *Brain Topography*, vol. 25, no. 1, pp. 20–26, Jan. 2012.
- [35] L. Bréchet, D. Brunet, G. Birot, R. Gruetter, C. M. Michel, and J. Jorge, "Capturing the spatiotemporal dynamics of self-generated, task-initiated thoughts with EEG and fMRI," *NeuroImage*, vol. 194, pp. 82–92, Jul. 2019.

- [36] A. Damborská, C. Pigué, J.-M. Aubry, A. G. Dayer, C. M. Michel, and C. Berchio, "Deviant EEG resting-state large-scale brain network dynamics in euthymic bipolar disorder patients," *Frontiers Psychiatry*, vol. 10, p. 826, Nov. 2019.
- [37] B. Ross, T. Miyazaki, J. Thompson, S. Jamali, and T. Fujioka, "Human cortical responses to slow and fast binaural beats reveal multiple mechanisms of binaural hearing," *J. Neurophysiol.*, vol. 112, no. 8, pp. 1871–1884, 2014.
- [38] J. C. R. Licklider, J. C. Webster, and J. M. Hedlun, "On the frequency limits of binaural beats," *J. Acoust. Soc. Amer.*, vol. 22, no. 4, pp. 468–473, Jul. 1950.
- [39] T. Seifi Ala, M. A. Ahmadi-Pajouh, and A. M. Nasrabadi, "Cumulative effects of theta binaural beats on brain power and functional connectivity," *Biomed. Signal Process. Control*, vol. 42, pp. 242–252, Apr. 2018.
- [40] M. Garcia-Argibay, M. A. Santed, and J. M. Reales, "Binaural auditory beats affect long-term memory," *Psychol. Res.*, vol. 83, no. 6, pp. 1124–1136, Dec. 2017.
- [41] B. Hommel, R. Sellaro, R. Fischer, S. Borg, and L. S. Colzato, "High-frequency binaural beats increase cognitive flexibility: Evidence from dual-task crosstalk," *Frontiers Psychol.*, vol. 7, p. 1287, Aug. 2016.
- [42] P. A. McConnell, B. Froeliger, E. L. Garland, J. C. Ives, and G. A. Sforzo, "Auditory driving of the autonomic nervous system: Listening to theta-frequency binaural beats post-exercise increases parasympathetic activation and sympathetic withdrawal," *Frontiers Psychol.*, vol. 5, p. 1248, Nov. 2014.
- [43] M. Wu and Z.-H. Meng, "Just noticeable difference of duration perception and influence factors of different noise," *Audio Eng.*, vol. 43, no. 8, pp. 15–16, Jul. 2019.
- [44] C. Beauchene, N. Abaid, R. Moran, R. A. Diana, and A. Leonessa, "The effect of binaural beats on visuospatial working memory and cortical connectivity," *PLoS ONE*, vol. 11, no. 11, Nov. 2016, Art. no. e0166630.
- [45] J. Martinovic and N. A. Busch, "High frequency oscillations as a correlate of visual perception," *Int. J. Psychophysiol.*, vol. 79, no. 1, pp. 32–38, Jan. 2011.
- [46] N. A. Busch, C. S. Herrmann, M. M. Müller, D. Lenz, and T. Gruber, "A cross-laboratory study of event-related gamma activity in a standard object recognition paradigm," *NeuroImage*, vol. 33, no. 4, pp. 1169–1177, Dec. 2006.
- [47] K. Yang, L. Tong, J. Shu, N. Zhuang, B. Yan, and Y. Zeng, "High gamma band EEG closely related to emotion: Evidence from functional network," *Frontiers Human Neurosci.*, vol. 14, p. 89, Mar. 2020.
- [48] M. K. Rieder, B. Rahm, J. D. Williams, and J. Kaiser, "Human gamma-band activity and behavior," *Int. J. Psychophysiol.*, vol. 79, no. 1, pp. 39–48, Jan. 2011.
- [49] S. Aydın, "Cross-validated AdaBoost classification of emotion regulation strategies identified by spectral coherence in resting-state," *Neuroinformatics*, pp. 1–13, Sep. 2021, doi: 10.1007/s12021-021-09542-7.
- [50] M. M. Murray, D. Brunet, and C. M. Michel, "Topographic ERP analyses: A step-by-step tutorial review," *Brain Topography*, vol. 20, no. 4, pp. 249–264, Mar. 2008.
- [51] F. von Wegner, P. Knaut, and H. Laufs, "EEG microstate sequences from different clustering algorithms are information-theoretically invariant," *Frontiers Comput. Neurosci.*, vol. 12, p. 70, Aug. 2018.
- [52] W. Friedrich, S. Du, and K. Balt, "Studying frequency processing of the brain to enhance long-term memory and develop a human brain protocol," *Technol. Health Care*, vol. 23, no. s2, pp. S465–S471, Jun. 2015.
- [53] Q. Chen, D. Wang, K. L. Shapiro, and S. Hanslmayr, "Using fast visual rhythmic stimulation to control inter-hemispheric phase offsets in visual areas," *Neuropsychologia*, vol. 157, Jul. 2021, Art. no. 107863.
- [54] V. Wespatat, "Phase sensitivity of synaptic modifications in oscillating cells of rat visual cortex," *J. Neurosci.*, vol. 24, no. 41, pp. 9067–9075, Oct. 2004.
- [55] P. Goodin, J. Ciorciari, K. Baker, A.-M. Carrey, M. Harper, and J. Kaufman, "A high-density EEG investigation into steady state binaural beat stimulation," *PLoS ONE*, vol. 7, no. 4, Apr. 2012, Art. no. e34789.
- [56] T. van Duijn, H. Crocket, and R. S. W. Masters, "The role of instruction preference in analogy learning: Brain activity and motor performance," *Psychol. Sport Exercise*, vol. 47, Mar. 2020, Art. no. 101615.
- [57] T. L. Blankenship and M. A. Bell, "Frontotemporal coherence and executive functions contribute to episodic memory during middle childhood," *Develop. Neuropsychol.*, vol. 40, nos. 7–8, pp. 430–444, Apr. 2016.
- [58] X. Lei and K. Liao, "Understanding the influences of EEG reference: A large-scale brain network perspective," *Front Neurosci.*, vol. 11, p. 205, Apr. 2017.
- [59] H. Siamaknejad, W. S. Liew, and C. K. Loo, "Fractal dimension methods to determine optimum EEG electrode placement for concentration estimation," *Neural Comput. Appl.*, vol. 31, no. 3, pp. 945–953, Sep. 2017.
- [60] C. Imperatori, B. Farina, M. I. Quintiliani, A. Onofri, P. C. Gattinara, M. Lepore, V. Gnoni, E. Mazzucchi, A. Contardi, and G. D. Marca, "Aberrant EEG functional connectivity and EEG power spectra in resting state post-traumatic stress disorder: A sLORETA study," *Biol. Psychol.*, vol. 102, pp. 10–17, Oct. 2014.
- [61] S. A. Reedijk, A. Bolders, L. S. Colzato, and B. Hommel, "Eliminating the attentional blink through binaural beats: A case for tailored cognitive enhancement," *Frontiers Psychiatry*, vol. 6, p. 82, Jun. 2015.
- [62] L. S. Colzato, H. Barone, R. Sellaro, and B. Hommel, "More attentional focusing through binaural beats: Evidence from the global–local task," *Psychol. Res.*, vol. 81, no. 1, pp. 271–277, Nov. 2015.
- [63] C. Beauchene, N. Abaid, R. Moran, R. A. Diana, and A. Leonessa, "The effect of binaural beats on verbal working memory and cortical connectivity," *J. Neural Eng.*, vol. 14, no. 2, Feb. 2017, Art. no. 026014.
- [64] C. Beauchene, N. Abaid, R. Moran, R. A. Diana, and A. Leonessa, "The effect of binaural beats on visuospatial working memory and cortical connectivity," *PLoS ONE*, vol. 11, no. 11, Nov. 2016, Art. no. e0166630.
- [65] S. Jafari, Z. Ansari, S. M. R. H. Golpayegani, and S. Gharibzadeh, "Is attention a 'period window' chaotic brain," *J. Neuropsychiatry Clin. Neurosci.*, vol. 25, no. 1, p. E05, Mar. 2013.
- [66] A. Accardo, M. Affinito, M. Carrozzini, and F. Bouquet, "Use of the fractal dimension for the analysis of electroencephalographic time series," *Biological*, vol. 77, no. 5, pp. 339–350, 1997.
- [67] P. Milz, P. L. Faber, D. Lehmann, T. Koenig, K. Kochi, and R. D. Pascual-Marqui, "The functional significance of EEG microstates—Associations with modalities of thinking," *NeuroImage*, vol. 125, pp. 643–656, Jan. 2016.
- [68] E. Pipinis, S. Melynyte, T. Koenig, L. Jarutyte, K. Linkenkaer-Hansen, O. Ruksenas, and I. Griskova-Bulanova, "Association between resting-state microstates and ratings on the Amsterdam resting-state questionnaire," *Brain Topography*, vol. 30, no. 2, pp. 245–248, Sep. 2016.
- [69] B. A. Seitzman, M. Abell, S. C. Bartley, M. A. Erickson, A. R. Bolbecker, and W. P. Hetrick, "Cognitive manipulation of brain electric microstates," *NeuroImage*, vol. 146, pp. 533–543, Feb. 2017.
- [70] P. Milz, R. D. Pascual-Marqui, P. Achermann, K. Kochi, and P. L. Faber, "The EEG microstate topography is predominantly determined by intracortical sources in the alpha band," *NeuroImage*, vol. 162, pp. 353–361, Nov. 2017.
- [71] J. Britz, D. Van De Ville, and C. M. Michel, "BOLD correlates of EEG topography reveal rapid resting-state network dynamics," *NeuroImage*, vol. 52, no. 4, pp. 1162–1170, Oct. 2010.
- [72] A. Custo, D. Van De Ville, W. M. Wells, M. I. Tomescu, D. Brunet, and C. M. Michel, "Electroencephalographic resting-state networks: Source localization of microstates," *Brain Connectivity*, vol. 7, no. 10, pp. 671–682, Dec. 2017.
- [73] Y. Cai, D. Huang, Y. Chen, H. Yang, C.-D. Wang, F. Zhao, J. Liu, Y. Sun, G. Chen, X. Chen, H. Xiong, and Y. Zheng, "Deviant dynamics of resting state electroencephalogram microstate in patients with subjective tinnitus," *Frontiers Behav. Neurosci.*, vol. 12, p. 122, Jun. 2018.
- [74] M. I. Tomescu, T. A. Rihs, R. Becker, J. Britz, A. Custo, F. Grouiller, M. Schneider, M. Debbané, S. Eliez, and C. M. Michel, "Deviant dynamics of EEG resting state pattern in 22q11.2 deletion syndrome adolescents: A vulnerability marker of schizophrenia?" *Schizophrenia Res.*, vol. 157, nos. 1–3, pp. 175–181, Aug. 2014.
- [75] M. Krylova, S. Alizadeh, I. Izyurov, V. Teckentrup, C. Chang, J. van der Meer, M. Erb, N. Kroemer, T. Koenig, M. Walter, and H. Jamalabadi, "Evidence for modulation of EEG microstate sequence by vigilance level," *NeuroImage*, vol. 224, Jan. 2021, Art. no. 117393.
- [76] C. Andreou, P. L. Faber, G. Leicht, D. Schoettle, N. Polomac, I. L. Hanganu-Opatz, D. Lehmann, and C. Mulert, "Resting-state connectivity in the prodromal phase of schizophrenia: Insights from EEG microstates," *Schizophrenia Res.*, vol. 152, nos. 2–3, pp. 513–520, Feb. 2014.
- [77] M. Kikuchi, T. Koenig, Y. Wada, M. Higashima, Y. Koshino, W. Strik, and T. Dierks, "Native EEG and treatment effects in neuroleptic-naïve schizophrenic patients: Time and frequency domain approaches," *Schizophrenia Res.*, vol. 97, nos. 1–3, pp. 163–172, 2007.
- [78] T. Sverak, L. Albrechtova, M. Lamos, I. Rektorova, and L. Ustohal, "Intensive repetitive transcranial magnetic stimulation changes EEG microstates in schizophrenia: A pilot study," *Schizophrenia Res.*, vol. 193, pp. 451–452, Mar. 2018.

- [79] L. Lei, Z. Liu, Y. Zhang, M. Guo, P. Liu, X. Hu, C. Yang, A. Zhang, N. Sun, Y. Wang, and K. Zhang, "EEG microstates as markers of major depressive disorder and predictors of response to SSRIs therapy," *Prog. Neuro-Psychopharmacol. Biol. Psychiatry*, vol. 116, Jun. 2022, Art. no. 110514.
- [80] L.-W. Ko, R. K. Chikara, Y.-C. Lee, and W.-C. Lin, "Exploration of user's mental state changes during performing brain-computer interface," *Sensors*, vol. 20, no. 11, p. 3169, Jun. 2020.



XINYUE LI is pursuing the B.S. degree in biomedical engineering with the Hebei University of Technology, Tianjin, China. Her current research interest includes neural engineering.



LEI WANG received the Ph.D. degree in theory and new technology of electrical engineering from the Hebei University of Technology, Tianjin, China, in 2009. He is currently the M.S. Supervisor and an Associate Professor with the Hebei University of Technology. His current research interests include neural engineering and brain science.



WEN ZHANG received the B.S. degree in biomedical engineering from the Taiyuan University of Technology, Taiyuan, China, in 2017. She is currently pursuing the M.S. degree with the Hebei University of Technology. Her current research interest includes neural engineering.



SHUO YANG received the Ph.D. degree in theory and new technology of electrical engineering from the Hebei University of Technology, Tianjin, China, in 2008. She is currently the Ph.D. Supervisor and a Professor with the Hebei University of Technology. Her current research interests include neural engineering and brain science.

...